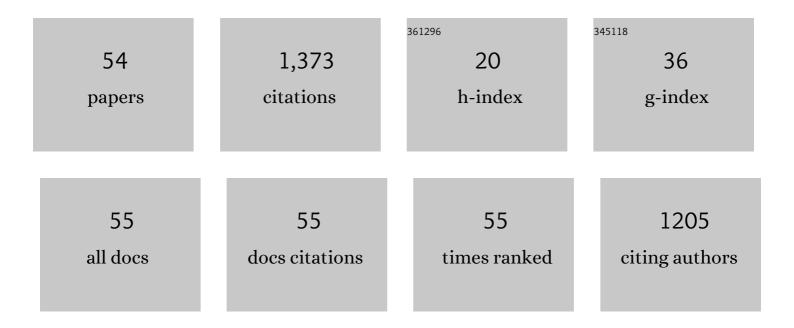
## **Christopher P Cheng**

List of Publications by Year in descending order

Source: https://exaly.com/author-pdf/3717507/publications.pdf Version: 2024-02-01



| #  | Article  | IF  | CITATIONS |
|----|--|-----|-----------|
| 1  | In Vivo MR Angiographic Quantification of Axial and Twisting Deformations of the Superficial Femoral<br>Artery Resulting from Maximum Hip and Knee Flexion. Journal of Vascular and Interventional<br>Radiology, 2006, 17, 979-987.              | 0.2 | 146       |
| 2  | Abdominal aortic hemodynamics in young healthy adults at rest and during lower limb exercise:<br>quantification using image-based computer modeling. American Journal of Physiology - Heart and<br>Circulatory Physiology, 2006, 291, H668-H676. | 1.5 | 120       |
| 3  | Quantification of Wall Shear Stress in Large Blood Vessels Using Lagrangian Interpolation Functions<br>with Cine Phase-Contrast Magnetic Resonance Imaging. Annals of Biomedical Engineering, 2002, 30,<br>1020-1032.                            | 1.3 | 96        |
| 4  | Methods for Quantifying Three-Dimensional Deformation of Arteries due to Pulsatile and<br>Nonpulsatile Forces: Implications for the Design of Stents and Stent Grafts. Annals of Biomedical<br>Engineering, 2009, 37, 14-33.                     | 1.3 | 87        |
| 5  | Abdominal aortic hemodynamic conditions in healthy subjects aged 50–70 at rest and during lower<br>limb exercise: in vivo quantification using MRI. Atherosclerosis, 2003, 168, 323-331.   | 0.4 | 79        |
| 6  | Inferior vena caval hemodynamics quantified in vivo at rest and during cycling exercise using<br>magnetic resonance imaging. American Journal of Physiology - Heart and Circulatory Physiology, 2003,<br>284, H1161-H1167.                       | 1.5 | 73        |
| 7  | The Effect of Aging on Deformations of the Superficial Femoral Artery Resulting from Hip and Knee<br>Flexion: Potential Clinical Implications. Journal of Vascular and Interventional Radiology, 2010, 21,<br>195-202.                           | 0.2 | 70        |
| 8  | Hemodynamic Changes Quantified in Abdominal Aortic Aneurysms with Increasing Exercise Intensity<br>Using MR Exercise Imaging and Image-Based Computational Fluid Dynamics. Annals of Biomedical<br>Engineering, 2011, 39, 2186-2202.             | 1.3 | 70        |
| 9  | Quantification of Particle Residence Time in Abdominal Aortic Aneurysms Using Magnetic Resonance<br>Imaging and Computational Fluid Dynamics. Annals of Biomedical Engineering, 2011, 39, 864-883.   | 1.3 | 67        |
| 10 | Geometry and respiratory-induced deformation of abdominal branch vessels and stents after complex endovascular aneurysm repair. Journal of Vascular Surgery, 2015, 61, 875-885.  | 0.6 | 45        |
| 11 | Blood flow conditions in the proximal pulmonary arteries and vena cavae: healthy children during<br>upright cycling exercise. American Journal of Physiology - Heart and Circulatory Physiology, 2004, 287,<br>H921-H926.                        | 1.5 | 41        |
| 12 | Proximal pulmonary artery blood flow characteristics in healthy subjects measured in an upright posture using MRI: The effects of exercise and age. Journal of Magnetic Resonance Imaging, 2005, 21, 752-758.                                    | 1.9 | 41        |
| 13 | Comparison of abdominal aortic hemodynamics between men and women at rest and during lower limb exercise. Journal of Vascular Surgery, 2003, 37, 118-123.  | 0.6 | 35        |
| 14 | Right Renal Artery In Vivo Stent Fracture. Journal of Vascular and Interventional Radiology, 2008, 19, 439-442.  | 0.2 | 33        |
| 15 | In Vivo Deformation of the Human Abdominal Aorta and Common Iliac Arteries With Hip and Knee<br>Flexion: <b>Implications for the Design of Stent-Grafts</b> . Journal of Endovascular Therapy, 2009, 16,<br>531-538.                             | 0.8 | 33        |
| 16 | Aortic Arch Vessel Geometries and Deformations in Patients with Thoracic Aortic Aneurysms and Dissections. Journal of Vascular and Interventional Radiology, 2014, 25, 1903-1911.  | 0.2 | 29        |
| 17 | Respiration-induced Deformations of the Superior Mesenteric and Renal Arteries in Patients with<br>Abdominal Aortic Aneurysms. Journal of Vascular and Interventional Radiology, 2013, 24, 1035-1042.  | 0.2 | 26        |
| 18 | Comparative geometric analysis of renal artery anatomy before and after fenestrated or snorkel/chimney endovascular aneurysm repair. Journal of Vascular Surgery, 2016, 63, 922-929.   | 0.6 | 25        |

CHRISTOPHER P CHENG

| #  | Article  | IF  | CITATIONS |
|----|--|-----|-----------|
| 19 | Relative Lung Perfusion Distribution in Normal Lung Scans: Observations and Clinical Implications.<br>Congenital Heart Disease, 2006, 1, 210-216.  | 0.0 | 24        |
| 20 | Changes in Geometry and Cardiac Deformation of the Thoracic Aorta after Thoracic Endovascular<br>Aortic Repair. Annals of Vascular Surgery, 2018, 46, 83-89.   | 0.4 | 23        |
| 21 | Dynamic exercise imaging with an MR-compatible stationary cycle within the general electric open magnet. Magnetic Resonance in Medicine, 2003, 49, 581-585.  | 1.9 | 21        |
| 22 | Three-Dimensional Modeling Analysis of Visceral Arteries and Kidneys during Respiration. Annals of<br>Vascular Surgery, 2016, 34, 250-260.   | 0.4 | 20        |
| 23 | Biomechanical Response of Stented Carotid Arteries to Swallowing and Neck Motion. Journal of Endovascular Therapy, 2008, 15, 663-671.  | 0.8 | 17        |
| 24 | The biomechanical impact of hip movement on iliofemoral venous anatomy and stenting for deep venous thrombosis. Journal of Vascular Surgery: Venous and Lymphatic Disorders, 2020, 8, 953-960.   | 0.9 | 16        |
| 25 | Dynamic Geometric Analysis of the Renal Arteries and Aorta following Complex Endovascular<br>Aneurysm Repair. Annals of Vascular Surgery, 2017, 43, 85-95.   | 0.4 | 13        |
| 26 | Geometric Deformations of the Thoracic Aorta and Supra-Aortic Arch Branch Vessels Following<br>Thoracic Endovascular Aortic Repair. Vascular and Endovascular Surgery, 2018, 52, 173-180.  | 0.3 | 13        |
| 27 | Respiratoryâ€induced 3D deformations of the renal arteries quantified with geometric modeling during<br>inspiration and expiration breathâ€holds of magnetic resonance angiography. Journal of Magnetic<br>Resonance Imaging, 2013, 38, 1325-1332. | 1.9 | 12        |
| 28 | Methods for Characterizing Human Coronary Artery Deformation From Cardiac-Gated Computed<br>Tomography Data. IEEE Transactions on Biomedical Engineering, 2014, 61, 2582-2592.   | 2.5 | 12        |
| 29 | Optimization of three-dimensional modeling for geometric precision and efficiency for healthy and diseased aortas. Computer Methods in Biomechanics and Biomedical Engineering, 2018, 21, 65-74.   | 0.9 | 9         |
| 30 | Influence of thoracic endovascular aortic repair on true lumen helical morphology for Stanford<br>type B dissections. Journal of Vascular Surgery, 2021, 74, 1499-1507.e1.   | 0.6 | 9         |
| 31 | Quantifying in vivo hemodynamic response to exercise in patients with intermittent claudication and abdominal aortic aneurysms using cine phaseâ€contrast MRI. Journal of Magnetic Resonance Imaging, 2010, 31, 425-429.                           | 1.9 | 8         |
| 32 | Thoracic aortic geometry correlates with endograft bird-beaking severity. Journal of Vascular<br>Surgery, 2020, 72, 1196-1205.   | 0.6 | 7         |
| 33 | Multiaxial pulsatile dynamics of the thoracic aorta and impact of thoracic endovascular repair.<br>European Journal of Radiology Open, 2021, 8, 100333.  | 0.7 | 7         |
| 34 | Respiratory-induced changes in renovisceral branch vessel morphology after fenestrated<br>thoracoabdominal aneurysm repair with the BeGraft balloon-expandable covered stent. Journal of<br>Vascular Surgery, 2021, 74, 396-403.                   | 0.6 | 6         |
| 35 | Stabilization of the Abdominal Aorta During the Cardiac Cycle with the Sac-Anchoring Nellix Device.<br>Annals of Vascular Surgery, 2018, 52, 312.e7-312.e12.   | 0.4 | 5         |
| 36 | Automated Quantification of Diseased Thoracic Aortic Longitudinal Centerline and Surface<br>Curvatures. Journal of Biomechanical Engineering, 2020, 142, .   | 0.6 | 5         |

CHRISTOPHER P CHENG

| #  | Article  | IF  | CITATIONS |
|----|--|-----|-----------|
| 37 | Abdominal Aortic Hemodynamics in Intermittent Claudication Patients at Rest and during Dynamic<br>Pedaling Exercise. Annals of Vascular Surgery, 2015, 29, 1516-1523.  | 0.4 | 4         |
| 38 | If You Build It, They Will Come: How to Establish an Academic Innovation Enterprise. Techniques in<br>Vascular and Interventional Radiology, 2017, 20, 121-126.  | 0.4 | 3         |
| 39 | Length Redundancy and Twist Improve the Biomechanical Properties of Polytetrafluoroethylene<br>Bypass Grafts. Annals of Vascular Surgery, 2019, 61, 410-415.   | 0.4 | 3         |
| 40 | Cardiac Pulsatility– and Respiratory-Induced Deformations of the Renal Arteries and Snorkel Stents<br>After Snorkel Endovascular Aneurysm Sealing. Journal of Endovascular Therapy, 2019, 26, 556-564.       | 0.8 | 3         |
| 41 | Thoracic aortic parallel stent-graft behaviour when subjected to radial loading. Journal of the<br>Mechanical Behavior of Biomedical Materials, 2021, 118, 104407.   | 1.5 | 3         |
| 42 | Quantification of motion of the thoracic aorta after ascending aortic repair of type-A dissection.<br>International Journal of Computer Assisted Radiology and Surgery, 2017, 12, 811-819.                   | 1.7 | 2         |
| 43 | Geometric Modeling of Vasculature. , 2019, , 45-66.  |     | 2         |
| 44 | Quantification of true lumen helical morphology and chirality in type B aortic dissections. American<br>Journal of Physiology - Heart and Circulatory Physiology, 2021, 320, H901-H911.                      | 1.5 | 2         |
| 45 | Hemodynamics in Human Abdominal Aortic Aneurysms During Rest and Simulated Exercise. , 2007, , .   |     | 2         |
| 46 | Quantification of In Vivo Kinematics of Superficial Femoral Artery due to Hip and Knee Flexion Using<br>Magnetic Resonance Imaging. Journal of Medical and Biological Engineering, 2016, 36, 80-86.          | 1.0 | 1         |
| 47 | Coronary Arteries and Heart. , 2019, , 87-116.   |     | 1         |
| 48 | Effects of Heat Treatment on the Magnetic Properties of Nitinol Devices. Shape Memory and Superelasticity, 2019, 5, 429-435.   | 1.1 | 1         |
| 49 | The Triple Wire Technique for Delivery of Endovascular Components in Difficult Anatomy. Annals of Vascular Surgery, 2021, 70, 197-201.   | 0.4 | 1         |
| 50 | Methods for Quantifying Vessel Deformation Due to Pulsatile and Non-Pulsatile Forces. , 2007, , .  |     | 1         |
| 51 | Impact of renal chimney intra-aortic stent length on branch and end-stent angle in chimney<br>endovascular aneurysm repair and endovascular aneurysm sealing configurations. Vascular, 2023, 31,<br>234-243. | 0.4 | 1         |
| 52 | Quantifying Vascular Deformations. , 2019, , 67-84.  |     | 0         |
| 53 | Thoracic Aorta and Supra-Aortic Arch Branches. , 2019, , 139-163.  |     | 0         |
| 54 | Abdominal Aorta and Renovisceral Arteries. , 2019, , 165-189.  |     | 0         |